Printing Floating-Point Numbers

A Faster, Always Correct Method

Marc Andrysco
University of California, San Diego, USA
andrysco@cs.ucsd.edu

Ranjit Jhala
University of California, San Diego, USA
jhala@cs.ucsd.edu

Sorin Lerner
University of California, San Diego, USA
lerner@cs.ucsd.edu

Abstract

Floating-point numbers are an essential part of modern software, recently gaining particular prominence on the web as the exclusive numeric format of Javascript. To use floating-point numbers, we require a way to convert binary machine representations into human readable decimal outputs. Existing conversion algorithms make trade-offs between completeness and performance. The classic Dragon4 algorithm by Steele and White and its later refinements achieve completeness — *i.e.* produce correct and optimal outputs on all inputs — by using arbitrary precision integer (bignum) arithmetic which leads to a high performance cost. On the other hand, the recent Grisu3 algorithm by Loitsch shows how to recover performance by using native integer arithmetic but sacrifices optimality for 0.5% of all inputs. We present Errol, a new complete algorithm that is guaranteed to produce correct and optimal results for all inputs by sacrificing a speed penalty of 2.4× to the incomplete Grisu3 but 5.2× faster than previous complete methods.

Categories and Subject Descriptors I.m [*Computing Methodologies*]: Miscellaneous

Keywords floating-point printing, dtoa, double-double

1. Introduction

How should we print a floating-point number? Consider the following curious interaction with a recent Python REPL (v2.7.5)

```
>>> 0.1 + 0.11
0.21000000000000002
```

The same counter-intuitive result is displayed by REPLs for JavaScript (`node.js` v0.10.30), Haskell (`GHCi` v7.10.1) and Ocaml (`Ocaml` v4.01.0). This puzzling behavior could be explained by rounding errors at one of *two* places: the actual *computation* or, in the focus of this paper, the *printing* phase.

The goal of the printing phase is to convert the machine-level binary representation of a floating-point number into a human-readable decimal representation with *as few digits as needed* to communicate the desired binary value. The conversion process is complicated by the fact that the machine can only represent a finite subset of the real numbers. Each binary machine-representable number corresponds to the *set of* real numbers in an interval around itself. The "wrong" output `0.21000000000000002` and the "right" output `0.21` may fall inside the same interval, and thus have exactly the same machine representation, making it hard for the output procedure to distinguish between the two. Hence, printing floating-point numbers is a surprisingly difficult problem with a distinguished line of work dating back several decades.

In 1990, Steele and White published the first paper to precisely pin down what it means to correctly and optimally print a floating-point number [14]. Intuitively, a (decimal) output is *correct* if it belongs inside the *interval* represented by the corresponding (binary) input. Furthermore, an output is *optimal* if it has the smallest number of digits among all the numbers in the interval represented by the input. Steele and White [14] show a recipe for designing correct and optimal algorithms and instantiate it in the Dragon4 algorithm for printing floating-point numbers. Unfortunately, Dragon4 relied on large integer ("bignum") arithmetic, incurring a high performance cost. Several authors including [5] and [1] devised improvements which optimized various steps that required slow bignum computations, making Dragon4 suitable for adoption inside various language run-times where it remained for about two decades. (Consequently, we can rest assured that the quirky behavior in the REPLs above is due to rounding and not conversion errors.)

This state of affairs remained until 2010 when Florian Loitsch presented the Grisu3 algorithm. Grisu3 achieved dramatic (up to 12.5×) improvements in efficiency by *mostly* replacing bignum computations with native 64-bit arithmetic [10]. Unfortunately, the speedup came at a price. Grisu3 is *incomplete* in that for about 0.5% of all inputs, the algorithm produces correct but sub-optimal outputs, *i.e.* without the fewest number of digits. Loitsch showed how the sub-optimality could be detected at run-time, and in such cases the algorithm could revert to a slower but optimal Dragon4 conversion. As printing floating-point numbers is a performance critical issue in JavaScript engines, where all `numbers` are `floats`, Grisu3 was rapidly adopted by major browser engines including Chrome, Firefox and WebKit.

In this paper, we present Errol, a new algorithm for the output conversion of floating-point numbers that is *complete* and 5.2× faster than Dragon4. We achieve this via the following contributions.

- First, we generalize Grisu-style approximate conversion algorithms into framework parameterized by an abstract *high-precision* `HP` data-type that is used to compute a narrow (resp. wide) interval which provides over- (resp. under-) approximations of the optimal decimal (§ 3).
- Second, we instantiate the framework by implementing `HP` numbers using Knuth's double-double representation [9]. The resulting algorithm, Errol1, is efficient due to novel algorithms for the key arithmetic operations. Surprisingly, we show that

the double-double representation shrinks sub-optimality by an order of magnitude because Errol1 computes the narrow and wide intervals more precisely than Grisu3 (§ 4).

- Third, we show *empirically* that further precision is useless as the errors are due to *pathological* values that are guaranteed to fall outside the scope of Grisu-style approximate conversion. Guided by the data, we formally characterize the region containing such pathological values, allowing us to simply fall back on an exact conversion for such inputs. We find the resulting algorithm, Errol2, to be optimal on 99.9999999% of all inputs (§ 5).
- Fourth, even outside the pathological space, Grisu-style approximation *may* yield sub-optimal results. We develop a novel *necessary condition* for an input to yield sub-optimal outputs and use it to develop a *constraint-based synthesis* algorithm that efficiently pre-computes all (141) inputs where Errol2 may yield the sub-optimal conversion. This tabulation yields Errol3 which is *guaranteed* to return correct and optimal conversion for all inputs (§ 6).
- Finally, we present an empirical evaluation comparing Errol3 against the state of the art. We show that it is $2.5\times$ slower than an incomplete Grisu3, $2.4\times$ slower than Grisu3 made complete via dynamic checking, and $5.2\times$ faster than Dragon4, the previous complete conversion method (§ 7).

2. Preliminaries

We begin with some preliminaries about the properties of floating-point numbers and their representation that are needed to understand our algorithm for output conversion.

2.1 Representation

Machines use floating-point number representations to approximate real number computations.

Floating-Point Representations. A *real* is a value on the real number line. A floating-point format defines a *finite* set of *representable* numbers (or just *representations*) where each representation covers a wide range (*i.e.* interval) of the real number line. Variables that name representations will always be adorned with a hat, such as $\hat{v}$, and are denoted with the type `FP`. Note that unlike integers, which have equal-width gaps between numbers, floating-point representations have a large range of possible gaps with small representations closely packed together and large representations spread far apart.

High-Precision Representations. A *high-precision* floating-point number refers to a custom format with higher precision than representations supported by the native machine's architecture. Variables for high-precision numbers are adorned with a tilde, such as $\tilde{v}$, and are denoted with the type `HP`. High-precision numbers can be implemented in a variety of ways, *e.g.* big-integers libraries or structures.

IEEE-754. `FP` representations consist of a fixed *radix* (or base), a fixed-width *significand*, and a fixed-width *exponent* of the form:

$$significand \times radix^{exponent}$$

The *significand* consists of a sequence of N digits $d_1 \ldots d_N$ where each digit d_i is in the range defined by the radix: $0 \leq d_i < radix$. The IEEE-754 standard defines a set of floating-point formats, including the ubiquitous double-precision (`double`) and single-precision (`float`) binary formats. For the sake of simplicity, the remainder of the paper will exclusively discuss `double` numbers unless otherwise specified.

Normal Representations. A single number can be represented by multiple floating-point representations; *e.g.* 0.12×10^2 and 1.2×10^1 represent the same decimal number. A *normal representation* is a floating-point number where there is a single, non-zero digit left of the radix point. Each floating-point number has a unique normal representation; *e.g.* 1.2×10^1 is the unique normal representation of the above number. However, the normal representation does not offer sufficient coverage for very small values close to zero. To expand the range of representable small numbers and enable "gradual underflow", the IEEE-754 standard defines the notion of a *subnormal* number where the $significand$ begins with a leading 0 bit followed by several lower order bits.

2.2 Conversion

As the `FP` numbers are finite, an arbitrary real number is unlikely to fall exactly upon an `FP` value. Next, we describe how reals are rounded to `FP` values in the IEEE-754 standard, and the notion of rounding to define correct and optimal conversion from floating point to decimal format.

Neighbors. For each representation $\hat{v}$ (except at the extremes) there exists a *successor* representation denoted as $\hat{v}^+$ which is the next (larger) representation, and a *predecessor* representation denoted as $\hat{v}^-$ which is the previous (smaller) representation. Thus, for each *real* number there is a pair of adjacent *neighbors* $\hat{v}$ and $\hat{v}^+$ such that the real is in the interval between the neighbors.

Midpoints. A *midpoint* $\tilde{m}$ is the real value exactly between two adjacent representations. Formally, for a representation $\hat{v}$, we define the *succeeding* and *preceeding* midpoints respectively as:

$$\tilde{m}^+ \doteq \frac{\hat{v} + \hat{v}^+}{2} \qquad \tilde{m}^- \doteq \frac{\hat{v}^- + \hat{v}}{2}$$

The midpoints are *not* representable using the native representation format but can be represented by most high-precision representations that provide at least a single additional bit.

Rounding: Intervals & Functions. Recall that a given value $\hat{v}$ is surrounded by the midpoints $\tilde{m}^-$ and $\tilde{m}^+$. Any real r in the range $\tilde{m}^- < r < \tilde{m}^+$ is rounded to $\hat{v}$. If the real falls exactly *on* a midpoint between two floating-point numbers, the standard dictates that the value must be rounded to the *even* floating-point number, [1]which is the number whose last bit is 0 (as opposed to *odd* numbers whose last bit is 1). Thus, the *rounding interval* of a binary representation $\hat{v}$ is the range $[\tilde{m}^-, \tilde{m}^+]$ when $\hat{v}$ is even or $(\tilde{m}^-, \tilde{m}^+)$ when $\hat{v}$ is odd. The *rounding function* flt takes a real number and rounds it to the nearest floating-point representation. Thus, for any number r in the rounding interval of $\hat{v}$, $\text{flt}(r) \doteq \hat{v}$.

Conversion: Correctness & Optimality. Let $\hat{v}$ be a *binary* input representation and let r be the *decimal* number produced as the conversion output. The conversion from $\hat{v}$ to r is *correct* if r falls in *rounding interval* of $\hat{v}$ (*i.e.* $\text{flt}(r) = \hat{v}$). The *length* of a real r is the number of decimal digits required to write the significand as a string. For example, the length of 1.24×10^5 is 3. The conversion from $\hat{v}$ to r is *optimal* if r is the value in the rounding interval of $\hat{v}$ with the smallest length, *i.e.* if every value in the rounding interval of $\hat{v}$ has length at least as large as r. Note that there may exist multiple, unique values of r of optimal length.

3. A Generic Conversion Framework

Our work builds on the Grisu3 algorithm of Loitsch [10]. In this section, we distill the insights from Grisu3 into a general conversion framework parameterized by an abstract high-precision representation `HP` and discuss the requirements on `HP` that ensure cor-

[1] IEEE-754 defines a set of five rounding modes; however, we focus only on round to nearest, ties to even

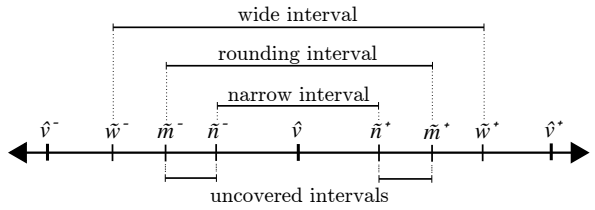

Figure 1: Representations, Midpoints and Boundaries: $\hat{v}$ denotes a native, machine representable floating point number with neighbors $\hat{v}^-$ and $\hat{v}^+$; $\tilde{m}^-$ and $\tilde{m}^+$ denote exact midpoints; $\tilde{n}^-$ and $\tilde{n}^+$ denote the narrow (or conservative) boundaries; $\tilde{w}^-$ and $\tilde{w}^+$ denote wide boundaries; and the uncovered intervals denote the portion of the rounding interval not covered by the narrow interval.

rectness and optimality. In § 4, we instantiate the framework with a novel `HP` type that is more accurate although slower than Grisu3.

3.1 Generic Conversion Algorithm

Recall that a correct and optimal decimal conversion of a number $\hat{v}$ is the shortest decimal in the rounding interval of $\hat{v}$. The key insight in Grisu3, illustrated in Figure 1, is to:

- *Step 1:* Compute narrow boundaries $\tilde{n}^-, \tilde{n}^+$ such that:
$$\tilde{m}^- < \tilde{n}^- < \hat{v} < \tilde{n}^+ < \tilde{m}^+$$
- *Step 2:* Compute shortest decimal in the interval $[\tilde{n}^-, \tilde{n}^+]$.

By relaxing the constraints of using *exact* midpoints $\tilde{m}^-, \tilde{m}^+$, Grisu3 can use efficient operations over limited-precision numbers (instead of Dragon4's bignum) to yield provably correct albeit possibly *suboptimal* conversions.

Scaled Narrow Intervals. A triple $(e, \bar{n}^-, \bar{n}^+)$ is a *scaled narrow interval* for $\hat{v}$ if there exists $\tilde{n}^-, \tilde{n}^+$ such that:

1. $\bar{n}^+ \in (1, 10]$
2. $\bar{n}^- \approx 10^{-e} \times \tilde{n}^-$
3. $\bar{n}^+ \approx 10^{-e} \times \tilde{n}^+$
4. $\tilde{m}^- < \tilde{n}^- < \hat{v} < \tilde{n}^+ < \tilde{m}^+$

Intuitively, a scaled narrow interval for $\hat{v}$ corresponds to a narrow interval for $\hat{v}$ where the boundaries are scaled by 10^{-e} to ensure that the upper bound $\bar{n}^+$ is in $(1, 10]$. Note that the last requirement allows us to compute the (scaled) narrow intervals approximately, *e.g.* using `HP` numbers, as long as the (unscaled) boundaries reside within the *exact* midpoints $\tilde{m}^-$ and $\tilde{m}^+$. Finally, only the upper boundary $\bar{n}^+$ must be in the interval $(1, 10]$, hence we observe that the exponent is $e \approx \lfloor \log_{10} \tilde{n}^+ \rfloor$.

Algorithm. Figure 2 formalizes the above intuition in a generic algorithm to `convert` an input `FP` value $\hat{v}$ into decimal form comprising a pair of a *sequence of digits* $d_1, \ldots, d_N$ and an exponent e denoting the decimal value $0.d_1 \ldots d_N \times 10^e$. (Although this differs slightly from the *normal* format – with a leading non-zero digit – we can normalize by shifting the decimal point to the right.) The `convert` algorithm is split into two procedures, `narrow_interval` and `digits`, corresponding to the steps described above. The first phase `narrow_interval` begins with the input $\hat{v}$ and computes a scaled narrow interval $(e, \bar{n}^-, \bar{n}^+)$ for $\hat{v}$. The second phase `digits` uses the scaled narrow interval to compute the final output *digits* corresponding to the *shortest* decimal value within the scaled narrow interval $[\bar{n}^-, \bar{n}^+]$. Next, we describe the two steps in detail.

```
def convert(v̂):
    (e, n̄⁻, n̄⁺)  = narrow_interval(v̂)
    digits       = digits(n̄⁻, n̄⁺)
    return (digits, e)

def narrow_interval(v̂):
    (ñ⁻, ñ⁺)  = boundary(v̂)
    e         = floor(log10(ñ⁺))
    n̄⁻        = multiply(ñ⁻, 10^-e)
    n̄⁺        = multiply(ñ⁺, 10^-e)
    return (e, n̄⁻, n̄⁺)

def digits(n̄⁻, n̄⁺):
    digits = []
    repeat:
      (n̄⁻, d⁻) = next_digit(n̄⁻)
      (n̄⁺, d⁺) = next_digit(n̄⁺)
      digits.append(d⁺)
    until(d⁻ != d⁺)
    return digits

def next_digit(n̄):
    d = truncate(n̄)
    n̄ = multiply(n̄ - d, 10)
    return (n̄, d)
```

Figure 2: A Generic Conversion Algorithm

3.2 Step 1: Compute Narrow Interval

The first phase computes the scaled narrow interval $(e, \bar{n}^-, \bar{n}^+)$ for the input $\hat{v}$. First, the (unscaled) boundary $\tilde{n}^-, \tilde{n}^+$ is computed directly from the input $\hat{v}$ by the function `boundary`. Second, the exponent e is directly computed from the upper boundary $\tilde{n}^+$ by scaling it to ensure that its significand lies in the range $[1, 10)$. That is, the exponent e is computed as the value $\lfloor \log_{10} \tilde{n}^+ \rfloor$. Finally, using the exponent, the *scaled* narrow boundaries are computed by `multiply`ing the narrow boundaries by 10^{-e}.

The functions `boundary` and `multiply` are deliberately left abstract. However, any concrete implementations must take care to ensure that despite errors introduced by rounding and propagation, the overall output is indeed a valid narrow interval for $\hat{v}$. Consequently, the narrow boundaries computed by `boundary` are chosen in a conservative fashion – as shown in Figure 3 – so that despite any rounding and propagation errors, the results remain within the actual midpoints, and hence form a valid narrow interval.

3.3 Step 2: Compute Digits

Once we have calculated the scaled narrow interval and corresponding exponent e, we can extract the *digits* using Steele & White's method [14].

One approach would simply generate digits of the upper bound in the following manner. Recall that the upper bound is scaled to be of the form $d_1.d_2 \ldots d_N$ – a result of falling in the range $[1, 10)$. Thus, the leading digit is retrieved by simply truncating the value to an integer, leaving a *remainder* bound comprising the digits $0.d_2 \ldots d_N$. The remainder is multiplied by 10 to return it to the decimal format $d_2.d_3 \ldots d_N$. The process can be iteratively performed N times, until all decimal digits are exhausted and the remainder is zero.

While this process yields a *correct* result that is in the rounding interval of the input $\hat{v}$, it does not yield the *optimal* value with the

shortest digit sequence. To recover optimality, Steele & White [14] make clever use of the *lower* boundary $\tilde{n}^-$: they simultaneously perform the above extraction process on *both* boundaries, generating *two* sequences of digits: $d_1^+ d_2^+ \ldots$ and $d_1^- d_2^- \ldots$, and repeating the process until it finds the first pair of digits that *differ i.e.* the first k such that $d_k^- \neq d_k^+$. The sequence of digits that is then output is the upper sequence $0.d_1^+ d_2^+ ... d_k^+$ which is identical to the lower sequence *except* at the very last digit.

Looking at it another way, the algorithm iteratively generates the digits of the upper bound $\tilde{n}^+$, forming the sequence $(d_1^+, d_1^+.d_2^+, d_1^+.d_2^+ d_3^+, ...)$. The process terminates once the generated number falls within the rounding interval. Figure 4 visually shows this process for the sample boundaries $\tilde{n}^- = 1.212$ and $\tilde{n}^+ = 1.234$. In this example, the algorithm produces the correct and optimal number 1.23.

Theorem 1. *The function* `digits` $(\bar{n}^-, \bar{n}^+)$ *returns the optimal (shortest) decimal value in the interval* $[\bar{n}^-, \bar{n}^+]$.

By construction, the output digits are guaranteed to be *correct*: the sequence of *digits* is guaranteed to be less than $\bar{n}^+$ and the algorithm terminates once *digits* is greater than $\bar{n}^-$. To show that the generated digits are *optimal*, *i.e.* they are the shortest sequence between $\tilde{n}^-$ and $\tilde{n}^+$, we refer to Theorem 6.2 in [10].

3.4 Optimality Verification

The above process computes a decimal output that is both *correct* and *optimal* within *narrow* boundaries; however, the output is not necessarily optimal within the larger *rounding* interval. In particular, the *uncovered interval* depicted in Figure 1, may contain a shorter decimal than any in the narrow interval considered by `digits`, and hence `convert` may fail to generate the shortest possible decimal output in the rounding interval.

Loitsch's Grisu3 algorithm introduces an *a posteriori* optimality verification step. Grisu3 computes a second decimal output over the *wide* interval that is guaranteed *optimal* (or shorter) but not necessarily correct, as it includes points outside the rounding interval. Nevertheless, if the length of the original and second outputs are equal, then the original output *must* be optimal [10]. Of course, there may be shorter decimals inside the wide interval *but not* inside the rounding interval. In this case, the verification would produce a *false negative*, errantly claiming the output is sub-optimal.

4. Errol1: Fast & More Optimal

Our first contribution is the Errol1 conversion algorithm, which instantiates the generic `convert` (Figure 2) with a novel `HP` implementation that simultaneously improves the *accuracy* and *performance* of conversion. The performance benefits come from implementing `HP` numbers using Knuth's *double-double* representation [9] and by developing novel algorithms for efficiently performing the key operations over double-doubles that are needed for conversion. Surprisingly, the double-double representation also improves the accuracy of conversion as it lets Errol1 compute the narrow and wide intervals more accurately, thereby *shrinking* the uncovered intervals and *increasing* the likelihood that the shortest number in the narrow interval is indeed the optimal result.

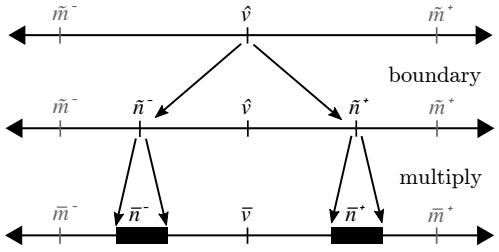

Figure 3: Error Propagation. The multiply operation computes the scaled interval $(\bar{n}^-, \bar{n}^+)$ with error (as represented by the black boxes), creating the requirement that the narrow interval $(\tilde{n}^-, \tilde{n}^+)$ be conservative enough to prevent overlap with the scaled midpoints $\bar{m}^-$ and $\bar{m}^+$

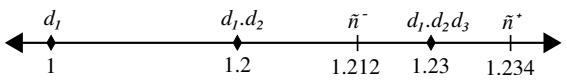

Figure 4: Correct and optimal digits generation. The lower bound is $\tilde{n}^- = 1.212$, and the upper bound is $\tilde{n}^+ = 1.234$. Diamonds denote the output digits at every iteration of the algorithm. The process generates the digits of $\tilde{n}^+$ one digit at a time, terminating once the output digits exceed the previous bound.

Real Number	0.2
8-bit FP Repr.	$1.10011_b \times 2^{-3}$
8-bit FP Value	0.19921875
16-bit HP Repr.	$1.10011_b \times 2^{-3}$ (base) $1.10011_b \times 2^{-8}$ (offset)
16-bit HP Value	0.1999969482421875

Figure 5: Representing 0.2 in FP and HP

Next, we describe double-double based `HP` values (§ 4.1) and how Errol1 uses them to implement the key `narrow_interval` (§ 4.2) and `digits` (§ 4.3) procedures of Figure 2. These procedures require fast and accurate implementations of specific arithmetic operations over `HP` numbers (§ 4.4), and finally we show how we ensure accuracy in the presence of rounding error (§ 4.5). For the remainder of the paper, the `HP` type refers to double-double floating-point numbers.

4.1 Double-Double Representation

We represent double-double numbers (of type `HP`) as a *pair* of native floating-point values (of type `FP`). That is,

```
type HP = (FP, FP)
```

`HP` values are written as $\langle \hat{v}_b, \hat{v}_\delta \rangle$ where the first element $\hat{v}_b$ is a *base* value corresponding to the nearest approximation of the target `HP` value, and the second element $\hat{v}_\delta$ is an *offset* value corresponding to the difference between the target value and the base. Thus, the `HP` value $\tilde{v}$ represented by $\langle \hat{v}_b, \hat{v}_\delta \rangle$ is the sum:

$$\tilde{v} \doteq \hat{v}_b + \hat{v}_\delta$$

Our pair-based representation doubles the precision of the native representation (*e.g.* if the native `FP` has 53 bits of precision, then our `HP` has 106 bits of precision). Figure 5 shows how the real 0.2 is represented as a native 8-bit `FP` and as a 16-bit `HP` value; the latter approximates the real more faithfully.

Non-Overlapping Invariant. Let $\hat{v}_b$ and $\hat{v}_\delta$ be two p-bit `FP` values. We say that $\langle \hat{v}_b, \hat{v}_\delta \rangle$ is *non-overlapping* if $e_b \geq e_\delta + p$ where e_b and e_δ are the exponents of $\hat{v}_b$ and $\hat{v}_\delta$, respectively. This implies the weaker statement $|\hat{v}_b| > |\hat{v}_\delta| 2^{p-1}$ that relates the magnitudes of $\hat{v}_b$ and $\hat{v}_\delta$. Our algorithms maintain the invariant that in any `HP` value $\langle \hat{v}_b, \hat{v}_\delta \rangle$, the components $\hat{v}_b$ and $\hat{v}_\delta$ are non-overlapping to ensure the most faithful representation of the target real number.

```
1  def narrow_interval_hp(v̂):
2    # Phase 1: Exponent Estimation
3    (_, e2)  = frexp(v̂)              # e2 ≈ log2 v̂
4    e        = floor(e2*0.30103)     # e ≈ log10 v̂
5    t̃        = pow10lookup(e)        # t̃ ≈ 10^-e
6    v̄        = multiply(v̂, t̃)
7    while(10 <= v̄):
8      v̄  = v̄ / 10
9      e  = e + 1
10     t̃b = t̃b / 10
11   while(v̄ < 1):
12     v̄  = v̄ * 10
13     e  = e - 1
14     t̃b = t̃b * 10
15
16   # Phase 2: Boundary Computation
17   n̄⁻ = (v̄b, v̄δ + (v̂⁻ - v̂) * t̃b / (2 * ε))
18   n̄⁺ = (v̄b, v̄δ + (v̂⁺ - v̂) * t̃b / (2 * ε))
19
20   # Phase 3: Exponent Rectification
21   while(10 <= n̄⁺):
22     n̄⁻ = n̄⁻ / 10
23     n̄⁺ = n̄⁺ / 10
24     e  = e + 1
25   while(n̄⁺ < 1):
26     n̄⁻ = n̄⁻ * 10
27     n̄⁺ = n̄⁺ * 10
28     e  = e - 1
29   return (e, n̄⁻, n̄⁺)
```

Figure 6: Errol1: Computing the Scaled Narrow Interval.

4.2 Step 1: Compute Narrow Interval

The narrow interval computation, summarized in Figure 6, is split into three distinct phases: exponent estimation, boundary computation, and exponent rectification. Each phase uses various *HP* arithmetic operations. We defer the implementation of these operations and the errors they incur to § 4.4.

Phase 1: Exponent Estimation. Unlike the description in Figure 2, Errol1 first *estimates* the exponent directly from the input $\hat{v}$ *before computing the boundaries*. The estimate optimizes performance by allowing Errol1 to use a fast lookup table to avoid several slow multiplications (by 10). However, as the estimated exponent may be incorrect, it is later rectified in the third phase.

The initial exponent estimation is shown on lines 2-14. The exponent is directly estimated from the input $\hat{v}$: the `frexp` function returns the binary exponent and is scaled by $\log_{10} 2 \approx 0.30103$ to provide a rough estimation of $\log_{10} \hat{v}$. The value of 10^{-e} is stored as an *HP* value in a lookup table and retrieved on line 5. The values $\hat{v}$ (an *FP*) and 10^{-e} (an *HP*) are multiplied to produce a scaled input $\bar{v}$ (an *HP*) on line 6. At the end of line 6, the value $\bar{v}$ has been scaled by 10^{-e} (as stored in $\tilde{t}$).

The lookup table for 10^{-e} can only contain values in the range $[10^{-291}, 10^{308}]$ in order to prevent overflow or underflow of an *HP* value. Consequently, input values below 10^{-308} or above 10^{291} are *not* successfully scaled into the range $[1, 10)$. Instead, the two loops on lines 6-13 check and incrementally multiply or divide by ten in order to completely scale $\bar{v}$, by adjusting the exponent e and the *base* component of $\tilde{t}$; the offset is not used later.

Phase 2: Boundary Computation. The boundaries $\bar{n}^-$ and $\bar{n}^+$ are computed from the original input $\hat{v}$ and scaled input $\bar{v}$ on lines 17 and 18. Using the definition of the scaled upper boundary $\bar{n}^+$, its computation directly follows from the calculation

$$\begin{aligned}\bar{n}^+ \doteq \frac{\bar{v} + \bar{v}^+}{2} &= \frac{\hat{v} + \hat{v}^+}{2} \times 10^{-e} = \frac{2\hat{v} + \hat{v}^+ - \hat{v}}{2} \times 10^{-e} \\ &= \hat{v} \times 10^{-e} + \frac{\hat{v}^+ - \hat{v}}{2} \times 10^{-e} \\ &= \bar{v} + \frac{\hat{v}^+ - \hat{v}}{2} \times \hat{t}_b\end{aligned}$$

where the last equality arises as $\bar{v}$ and $\hat{t}_b$ are equal to $\hat{v} \times 10^{-e}$ and 10^{-e}, respectively. Typically, summing the first term ($\bar{v}$) and the second term would require a full addition between two *HP* numbers. However, the second term is *extremely small* compared to the first due to the small difference between $\hat{v}$ and $\hat{v}^+$ and so the second term can be directly added to the offset component $\hat{s}_\delta$. The same process applies to computing the lower boundary $\bar{n}^-$ by substituting the successor $\hat{v}^+$ with the predecessor $\hat{v}^-$.

Accounting for Error with ε. The equality above corresponds to the *exact* boundaries. To compute the *narrow* (or *wide* boundaries), the divisor of 2 is adjusted by a factor ε in order to narrow or widen the interval $[\bar{n}^-, \bar{n}^+]$. As ε determines the width of the narrow and wide intervals, its exact value depends on the worst-case error incurred when computing the scaled boundaries $\bar{n}^-$ and $\bar{n}^+$ (as illustrated informally in figure 3). In § 4.4, we analyze the errors, and in § 4.5, we show they yield a suitable ε.

Phase 3: Exponent Rectification. Although the scaled input $\bar{v}$ *is* guaranteed to be within the interval $[1, 10)$, the scaled upper boundary $\bar{n}^+$ *is not* guaranteed to fall within the interval $[1, 10)$. The code on lines 21-28 inspects the value of $\bar{n}^+$, multiplying or dividing by ten in order to scale it to the desired range. The lower bound $\bar{n}^-$ and exponent are adjusted accordingly. Consequently, we can show that:

After the exponent and narrow interval are fully adjusted, the scaling invariants from section 3.1 are satisfied: the scaled upper boundary $\bar{n}^+$ falls uniquely in the range $[1, 10)$; the exponent satisfies the equation $\bar{n}^+ = 10^{-e}\tilde{n}^+$; and the lower bound is scaled in the form $\bar{n}^- = 10^{-e}\tilde{n}^-$. Formally, we can show:

Theorem 2. *The function* `narrow_interval_hp`$(\hat{v})$ *returns a scaled narrow interval* $(e, \bar{n}^-, \bar{n}^+)$ *for* $\hat{v}$.

4.3 Step 2: Compute Digits

We extract the digits from the scaled narrow interval by using the method of Steele & White [14], specialized to our double-double *HP* representation, as summarized in Figure 7.

Truncation in lines 4 and 5 is performed *directly* on the base component of the boundary. Care must be taken in order to guarantee the accuracy of truncation. Recall that by construction, an *HP* value consists of a base component that *best approximates* the target value (as an *FP*) and a smaller offset component that accounts for the remainder (as a non-overlapping *FP*). In order for the offset to affect truncation, the base component *must be an integer*; any non-integer value indicates the *HP* value is too far from an integer for the offset component to affect truncation (otherwise the base component is *not the best approximation*). If the base is an integer, the offset can only affect the truncation if it is *negative*; the code on lines 8-13 checks and accounts for this case. The extracted digit is removed from the boundary (lines 6, 7, 10, and 13), and the boundary is multiplied by ten (lines 15 and 16) in order to prepare the next digit for extraction. Subtraction is performed on the base component $\hat{n}_b$; the offset is too small to be affected.

```
1  def get_digits_hp(ñ⁻,ñ⁺):
2    digits = []
3    repeat:
4      d⁻ = trunc(n̂_b⁻)
5      d⁺ = trunc(n̂_b⁺)
6      ñ⁻ = ñ⁻ - d⁻
7      ñ⁺ = ñ⁺ - d⁺
8      if((n̂_b⁻ == 0) && (n̂_δ⁻ < 0))
9          d⁻ = d⁻ - 1
10         ñ⁻ = ñ⁻ + 1
11     if((n̂_b⁺ == 0) && (n̂_δ⁺ < 0))
12         d⁺ = d⁺ - 1
13         ñ⁺ = ñ⁺ + 1
14     digits.append(d⁺)
15     ñ⁺ = ñ⁺ * 10
16     ñ⁻ = ñ⁻ * 10
17   until(d⁻ != d⁺)
18   return digits
```

Figure 7: Errol1 algorithm for generating digits based on the boundaries $\bar{n}^-$ and $\bar{n}^+$.

Thus, as before, we can show that `digits_hp` returns a correct and optimal decimal in the given narrow interval:

Theorem 3. *The function* `digits_hp(`$\bar{n}^-$`,` $\bar{n}^+$`)` *returns the optimal (shortest) decimal value in the interval* $[\bar{n}^-, \bar{n}^+]$.

4.4 Double-Double Arithmetic

The eagle-eyed reader will have noticed that Errol1 (*i.e.* the code in Figures 6 and 7) requires only the following arithmetic operations: (1) add-*HP*-to-*FP* (2) multiply-*HP*-by-*FP* (3) multiply-*HP*-by-10 (4) divide-*HP*-by-10 Next, we describe novel algorithms to implement these arithmetic operations, and provide a detailed error analysis by bounding the maximum error using the standard numerical analysis notion of machine epsilon ϵ (also known as "macheps" or "unit roundoff") [6]. In § 4.5, we will use the per-operation error bounds to derive a value for ε that yields Theorem 2. As our *HP* format has twice the precision of *FP* numbers, our error analysis will be measured in terms of ϵ^2 which is equivalent to the maximum round-off error of an *HP* number. In the sequel, for all operations, we write $\tilde{x}$ and $\tilde{z}$ to denote the *HP input* and *output* respectively.

(1) Add-HP-to-FP. In Errol1, we only sum an *HP* number $\tilde{x}$ with an *FP* number $\hat{y}$ that is *smaller* than $\tilde{x}$. While not used directly in figures 6 and 7, this procedure serves as a subroutine used in subsequent operations. The output $\tilde{z}$ is computed component-wise, using a *compensation* c inspired by the Kahan summation algorithm [8]:

$$\begin{aligned} \hat{z}_b &\doteq \text{flt}(\hat{x}_b + \hat{y}) \\ c &\doteq (\hat{z}_b - \hat{x}_b) - \hat{y} \\ \hat{z}_\delta &\doteq \text{flt}(\hat{x}_\delta - c) \end{aligned}$$

The base component $\hat{z}_b$ is the best approximation of the sum between the two *FP* numbers $\hat{x}_b$ and $\hat{y}$. The value c is a *backwards compensation* that restores the digits that are "lost" when rounding $\hat{z}_b$. Most importantly, the compensation c is computed *exactly* without incurring any rounding error. Then, the compensation is added into the offset $\hat{x}_\delta$ and rounded to the nearest *FP*. Figure 8 illustrates how the truncated digits are recovered by the compensation.

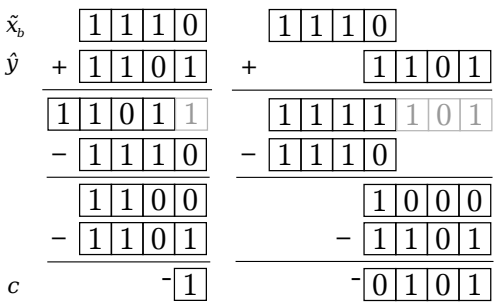

Figure 8: Example of computing the compensation c when summing together the FP numbers $\hat{x}_b$ and $\hat{y}$. The grey numbers correspond to digits that are discarded due to truncation. The left example shows two FP inputs that are nearly the same size where only a single bit is lost during truncation. The right example shows two inputs of very different size causing truncation of three bits, all of which are recovered.

Error Analysis. As the compensation c recovers all lost bits from the initial summation, the error of the addition operation lies *only* in the final rounding of $\hat{x}_\delta - c$. Thus, due to the non-overlapping invariant, the resulting error is at most ϵ^2 for the entire operation.

(2) Multiply-HP-by-FP. In Errol1 we need to multiply an *HP* number $\tilde{x}$ with an *FP* number $\hat{y}$, *e.g.* at line 6 of figure 6. By expanding the definition for *HP*, we can write the output $\tilde{z}$ as:

$$\begin{aligned} \tilde{z} &\doteq \tilde{x} \times \hat{y} = (\hat{x}_b + \hat{x}_\delta) \times \hat{y} \\ &= \hat{x}_b \times \hat{y} + \hat{x}_\delta \times \hat{y} \end{aligned} \tag{1}$$

The first multiplication is done using Knuth's method of splitting each p-bit `FP` number into two $\frac{p}{2}$-bit `FP` numbers and performing long-form multiplication, yielding an `HP` result *without error* [9]

$$\tilde{t} \doteq \hat{x}_b \times \hat{y} \tag{2}$$

Though the second term $\hat{x}_\delta \times \hat{y}$ can be also computed as an *HP* number, we can safely ignore the least-significant *FP* (*i.e.* the offset component), as this portion would almost entirely be lost when rounding the final $\tilde{z}$. Finally, the left term (an *HP*) and the right term (an *FP*) are added together using the previously described addition algorithm. The entire process is illustrated in Figure 9.

Error Analysis. There are three possible sources of error: the multiplication of the first term, the multiplication of the second term, and the final summation. The first term $\hat{x}_b \times \hat{y}$ in (1) is computed *without error*, as explained above. The second term $\hat{x}_\delta \times$

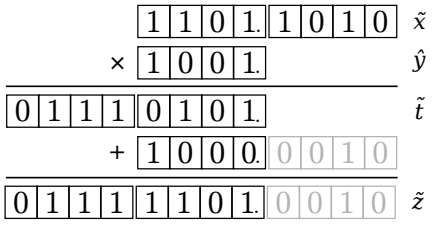

Figure 9: Example: Multiplying a 8-bit HP number $\tilde{x}$ with a 4-bit FP number $\hat{y}$. The base $\hat{x}_b$ is multiplied by $\hat{y}$ without error to produce the HP value $\tilde{t}$. The greyed values are omitted from the computation because they minimally affect the output $\tilde{z}$.

$\hat{y}$ in (1) is computed using native *FP* multiplication which incurs an error of ϵ. Due to non-overlapping, the components $\hat{x}_b$ and $\hat{x}_\delta$ must be related by $|\hat{x}_b| > |\hat{x}_\delta| 2^{p-1}$, and so:

$$|\hat{x}_b \hat{y}| > |\hat{x}_\delta \hat{y}| 2^{p-1}$$

Hence, $|\hat{x}_\delta \hat{y}|$ is smaller than the final output $\tilde{z}$ by a factor of 2^{-p+1} and so the total error caused by the second term is $\epsilon \times 2^{-p+1}$ or $2\epsilon^2$. Finally, the third source of error, the summation of the *HP* value $\tilde{t}$ to the unrounded *FP* $\hat{x}_\delta \times \hat{y}$, incurs an error of ϵ^2 as described above. Thus, in total, the multiply-*HP*-by-*FP* has relative error of $3\epsilon^2$.

(c) Multiply by 10. The procedure `get_digits_hp` (Figure 7) frequently uses multiply by 10 to shift the decimal point to the right. Each *FP* component (base and offset) is multiplied by 10:

$$\hat{h} \doteq \text{flt}(10 \times \hat{x}_b) \qquad \hat{l} \doteq \text{flt}(10 \times \hat{x}_\delta)$$

Rounding occurs for *both* operations; though it is tolerable for the lower product $\hat{l}$, rounding of $\hat{h}$ incurs a significant amount of error. Fortunately, the product is an addition of some bitshifts, the latter being multiplication by a power of two:

$$\hat{h} \doteq 10 \times \hat{x}_b = 8 \times \hat{x}_b + 2 \times \hat{x}_b$$

As in add-`HP`-to-`FP`, a compensated value c is backwards computed to recover the bits lost in the computation of $\hat{h}$ as an `FP` number:

$$c \doteq (\hat{h} - 8 \times \hat{x}_b) - 2 \times \hat{x}_b$$

Note that multiplication by 2 and 8 incurs no error so that the compensated value itself is computed without error. The final output $\tilde{z}$ integrates the compensation into the offset component:

$$\hat{z}_b \doteq \hat{h} \qquad \hat{z}_\delta \doteq \hat{l} - c$$

Error Analysis. Multiply-by-10 has three sources of error: computing $\hat{h}$, computing $\hat{l}$, and performing the final addition. First, computing $\hat{h}$ may incur error, but the lost bits are exactly recovered using compensation. Second, the error in $\hat{l}$ is at most ϵ; when accounting for the size of $\hat{l}$ compared to $\tilde{z}$, we have at most $2\epsilon^2$ of error. Third, the final addition incurs an additional ϵ^2 of error. Combined, multiply-by-10 incurs a maximum relative error of $3\epsilon^2$.

(d) Divide-by-10. Division follows a similar pattern to multiplication. First, both components are divided using native *FP* numbers:

$$\hat{h} \doteq \text{flt}(\hat{x}_b/10) \qquad \hat{l} \doteq \text{flt}(\hat{x}_\delta/10)$$

For multiplication, the `FP` value $\hat{h}$ was approximately ten times larger than $\hat{x}_b$; however for division, the *base component* $\hat{x}_b$ is ten times larger. Consequently, we compute the compensated value with respect to the *input* $\hat{x}_b$ (instead of the *output*):

$$c \doteq (\hat{x}_b - 8 \times \hat{h}) - 2 \times \hat{h}$$

As with multiplication, the compensation is computed *without error*. The compensated value c corresponds to the backwards difference between the *actual* and *exact* results multiplied by ten (*i.e.* between $10 \times \hat{h}$ and $10 \times h$). Notice that the exact error on the output satisfies $h - \hat{h} = c/10$. Unfortunately, division often produces numbers of infinite length that cannot be exactly represented by `FP` numbers. Consequently, the compensated value is rounded to the nearest `FP` value before being integrated into the result $\tilde{z}$:

$$\hat{z}_b \doteq \hat{h} \qquad \hat{z}_\delta \doteq \hat{l} - \text{flt}(c/10)$$

Error Analysis. Error occurs during three steps in the division operation: rounding of $\hat{l}$, rounding of $c/10$, and error during the final addition. As with the previous operations, rounding $\hat{l}$ incurs at most $2\epsilon^2$ error, and the final addition incurs ϵ^2 error. The rounding of the $c/10$ term produces an additional error on the order of ϵ^2. Combining all sources or error, divide-by-10 has a maximum relative error of $4\epsilon^2$.

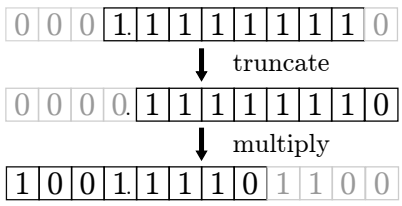

Figure 10: Worst-case error example when generating digits. The dark boxes correspond to an 8-bit floating-point number with a leading 1 bit. Grey boxes correspond to bits that the number cannot represent. Notice that are grey after the multiplication, indicating that they are lost due to truncation.

4.5 Ensuring Correctness under Rounding Errors

As shown in Figure 3, the maximum amount of error from the algorithm directly affects the selection of the narrow and wide bounds. The worst-case error for the entire Errol1 algorithm is found by summing the maximum error of every operation based on the worst-case run of the algorithm. We use this error to set ε to a value that ensures that the computed boundaries correctly lie within the actual midpoints.

Theorem 4 (Maximum Error)**.** *Given an FP format with a maximum round-off error of ϵ, the maximum relative error of for Errol1 using HP numbers is at most $79\epsilon^2$.*

Proof. From figure 6, there are four loops that are executed a variable number of times. The worst case for *small* numbers occurs for inputs below 10^{-323} where the lookup table can only perform an initial multiply of 10^{308}. The remaining factor 10^{15} requires 15 executions of the loop on lines 10-13 incurring a total error of $45\epsilon^2$. The worst case for *large* numbers occurs for values above 10^{308} where the lookup table can only perform an initial multiply of 10^{-291}. The remaining factor 10^{-17} requires 17 executions of the loop on lines 6-9 incurring a total error of $68\epsilon^2$. Because only a single loop is executed for a given input, the worse case error is the maximum of the two branches $68\epsilon^2$.

The remaining errors occur in three places: the operations used in exponent computation, a single ϵ^2 when computing the powers of ten lookup table, and a loss during digit generation. The digit generation portion of the algorithm loses at most 2 bits of precision (equivalent to $2\epsilon^2$). Future truncation and multiplications do not incur any errors: as digits are extracted, the number of bits shrink such that there is no further rounding. This process, graphically shown in figure 10, demonstrates a worst-case example where an input of all 1 bits is truncated and multiplied by ten to generate a number with two extra bits. Summing all sources of error, the maximum possible error from the entire algorithm is $79\epsilon^2$. □

Correctness. Next, we must set the ε to ensure that the bounds on lines 14 and 15 of Figure 6, are indeed correct (*i.e. narrow*). Setting ε to $n\epsilon$ accounts for $n\epsilon^2$ of error. Thus, for double-precision numbers with $\epsilon = 2^{-53}$, we define $\varepsilon \doteq 8.78 \times 10^{-15}$ which lets us ensure correctness, or formally, Theorem 2.

Optimality. Although Errol1 is *not* guaranteed to produce the shortest output, the narrow intervals provide a close enough approximation to the rounding interval that Errol1 is guaranteed to produce a decimal output with 17 digits or less.

Theorem 5. *(Maximum Length) The function* `convert_hp` $(\hat{v})$ *returns a decimal value with at most* 17 *digits.*

We prove this result using the analysis of Matula that provides an upper bound on the length required to uniquely print a number [11]. In particular, given a floating-point format with a radix b and p bits of precision, every number can be *uniquely* printed in decimal with $D = \lfloor n \log_{10} p \rfloor + 2$ digits. We can extend Matula's analysis to our setting (with narrow boundaries) to show that for double-precision floating-point numbers, every floating-point number can be correctly converted with no more than $D = 17$ digits.

Empirical Evaluation. By empirically running Errol1 on one billion inputs, we observed that *all* conversions were correct and 99.973% were *optimal* as compared to Grisu3's 99.5%. Thus, Errol1 is sub-optimal for an *order of magnitude fewer inputs* than Grisu3.

5. Errol2: Almost Optimal

Recall (from Figure 1) that Grisu3 and Errol1 return sub-optimal conversions if there is a number in the *uncovered* intervals that is *shorter* than the shortest number in the *narrow* interval. As Errol1 uses a more accurate `HP` format than Grisu3 (106-bits vs 64-bits), Errol1 is able to expand the size of the narrow interval and shrink the size of the uncovered intervals, thereby lowering the sub-optimality rate by an order of magnitude as smaller uncovered intervals are less likely to contain a shorter number. Surprisingly, we found that further expanding the narrow interval, *e.g.* by using even higher precision, *does not* improve optimality. Next, we describe how we *empirically* establish the above phenomenon (§ 5.1), *analytically* characterize the inputs where sub-optimal outputs are possible (§ 5.2), and how insights from the above yield Errol2, which is fast, correct and optimal on 99.9999999% of all inputs (§ 5.3).

5.1 Empirically Locating Optimality Failures

To empirically investigate the source of optimality failures, we randomly generated and converted one billion double-precision floating-point values and checked the results for optimality.

The Bad News: Pathological Midpoints. From the data, we observed the pattern that *every* observed failure was caused by a *pathological* midpoint ($\tilde{m}^-$ or $\tilde{m}^+$) whose length was shorter than *every* number inside the exclusive interval $(\tilde{m}^-, \tilde{m}^+)$. Because the midpoints are the most extreme points of the rounding interval, *any* narrowing – regardless of how precise – can *never* generate such numbers and hence, will not be optimal.

The Good News: Pathology is Contained. Fortunately, we discovered that the *distribution* of optimality failures forms a very unexpected and useful pattern. We split the space of inputs into 2098 bins where each bin had approximately 500,000 values drawn from the interval $[2^e, 2^{e+1})$. For every bin, we computed the percentage of optimality failures and show the results in Figure 11. Curiously, we found that pathological midpoints spike around $e = 58$ and exponentially decay as e goes to 0. Outside the range 2^{58} to 2^{82}, we observed *no optimality failures*.

5.2 Analytically Characterizing Optimality Failures

Next, we present a theoretical analysis that explains the curious spike, *i.e.* both the cause and location of pathological midpoints. First, we show that pathological midpoints *must be* integers, *i.e.* they have no bits right of the radix point. Second, we demonstrate that they become more rare as the values get larger; and after a certain point, the midpoints become so large that pathological cases become *extinct*. Consequently, for double-precision numbers, pathological midpoints must be integers in $[2^{54}, 2^{131}]$.

Theorem 6. *(Pathological Midpoints) If $\tilde{m}$ is a pathological midpoint then: (i) $\tilde{m}$ must be an integer, and (ii) $2^{54} \leq \tilde{m} \leq 2^{131}$.*

The proof of of the above requires a few basic definitions and facts about floating point numbers.

Index Decomposition. We say that d_i is the *digit at index* i in r when r is expressed in position notation. For example, when $r \doteq 3.1415$, we have $d_0 \doteq 3$ and $d_{-4} \doteq 5$, *i.e.* 3 and 5 are the digits at index 0 and -4 respectively. Thus, every real $r \doteq \sum_{k=-\infty}^{\infty} d_k 10^k$ where d_k is the digit at index k in r.

Leftmost & Rightmost Index. For finite-length numbers, let:

$$N(r) \doteq \max\{k \mid d_k \neq 0\} \qquad M(r) \doteq \min\{k \mid d_k \neq 0\}$$

We call $N(r)$ (resp. $M(r)$) the *left-most* (resp. *right-most*) index of r. The left-most index is exactly computable as: $N(r) \doteq \lfloor \log_{10} r \rfloor$. The right-most index is trickier in general but for integers is simply the number of trailing zeros, *i.e.* the maximum number of times the integer is evenly divisible by 10: $M(z) \doteq f_{10}(z)$ where $f_{10}(z)$ is the multiplicities of the factor 10 of z. For example, $M(12300) = f_{10}(12300) = 2$.

Length of a Number. The *length* of a real number $r \in \mathbb{R}$, written $L(r)$, is defined as: $L(r) \doteq N(r) - M(r) + 1$. Thus, $L(r)$ is the minimum number of digits necessary to write out the significand of r in decimal. Note that multiplication by (powers of) 10 does not effect a number's length; *i.e.* for any integer n, we have $L(r) = L(r \times 10^n)$. For example, $L(1.23) = L(1.23 \times 10^{-6}) = 3$.

Lemma 1. *(Shifting) In a floating-point format with p bits of precision, if $\hat{v}$ is a floating point number, and $\tilde{m}$ is a midpoint adjacent to $\hat{v}$ then there exists: (1) an integer e, (2) a natural number $z_{\hat{v}} < 2^{p+1}$ and (3) an odd natural number $2^{p+1} \leq z_{\tilde{m}} \leq 2^{p+2}$, such that: $\hat{v} = z_{\hat{v}} 2^e$ and $\tilde{m} = z_{\tilde{m}} 2^{e-1}$*

To see that $\hat{v} = z_{\hat{v}} 2^e$, we need only shift the binary significand of $\hat{v}$ at most p digits to the right until it is a natural. The fact that $z_{\tilde{m}}$ is odd follows from averaging two adjacent floating-point numbers $\hat{v}$ and $\hat{v}^+$ after writing them in the above shifted form; the average of two adjacent integers is an irreducible rational of the form $\frac{z_{\tilde{m}}}{2}$ and the factor two is incorporated into the 2^e term.

Proof of Theorem 6 (i): $\tilde{m}$ must be an Integer. We prove this case by contradiction. Suppose that midpoint $\tilde{m}$ is a non-integer rational *i.e.*, has a fractional component ($e < 0$). By Lemma 1, we have $\tilde{m} = z_{\tilde{m}} 2^{-e'}$ where $e' = -e$ is nonnegative. Hence

$$L(\tilde{m}) = L(z_{\tilde{m}} 2^{-e'}) = L(z_{\tilde{m}} \frac{10^{-e'}}{5^{-e'}}) = L(z_{\tilde{m}} 5^{e'})$$

where, by Lemma 1, $z_{\tilde{m}}$ is an odd integer. Because $5^{e'}$ is also odd, $z_{\tilde{m}} 5^{e'}$ must be odd, and therefore *not divisible* by 10. This implies that the right-most index $M(\tilde{m}) = 0$. Via the logarithmic form of N(r) we have

$$\begin{aligned} L(\tilde{m}) &= N(\tilde{m}) - M(\tilde{m}) + 1 \\ &= \lfloor \log_{10} z_{\tilde{m}} 5^{e'} \rfloor + 1 \end{aligned}$$

By Lemma 1 the natural $z_{\tilde{m}} \geq 2^{p+1}$, so:

$$L(\tilde{m}) \geq \lfloor (p+1) \log_{10} 2 + e' \log_{10} 5 \rfloor + 1$$

For double-precision floating-point numbers $p = 53$, so every non-integer midpoint has at least 17 digits. By the Maximum Length

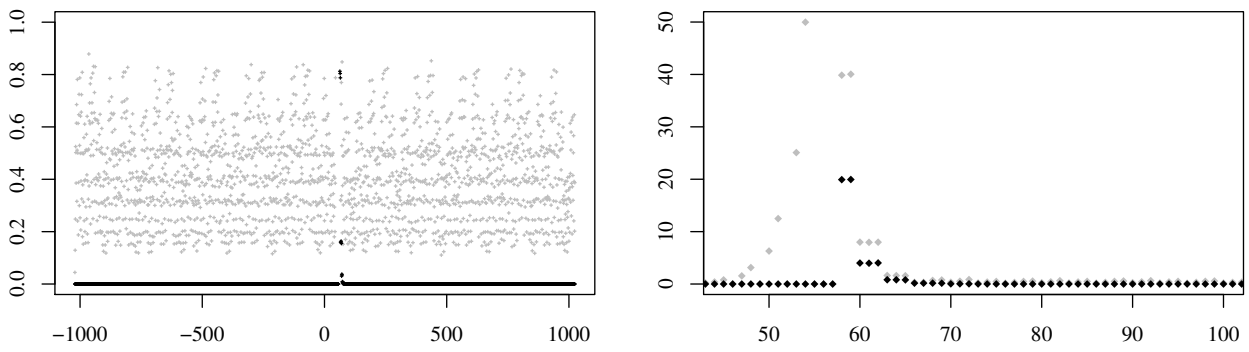

Figure 11: Optimality failures, with Errol1 in black and Grisu3 in grey. The x-axis represents binary exponents. For each exponent e on the x-axis, we randomly sample about $500,000$ values in the range $[2^e, 2^{e+1})$, and we plot along the y-axis, the percentage of those 500,000 values for which the conversion is suboptimal. The left plot shows that Errol1 has zero failures for nearly the entire input space (with an average of 0.027% failure rate) whereas Grisu3 fails consistently over the entire range (with an average of 0.5% failure rate). The left plot only shows the points with less than 1% error. The omitted points all fall in the range of exponents shown in the right plot, where we have focused the x-axis on these points and expanded the y-axis to see all the points above 1% error.

Theorem 5, Errol1 will produce an output of 17 digits or less, and so the non-integer midpoint $\tilde{m}$ *cannot be pathological*.

Proof of Theorem 6 (ii): $2^{54} \leq \tilde{m} \leq 2^{131}$. The lower bound $2^{54} \leq \tilde{m}$ follows as $\tilde{m}$ must be an integer. Recall that the rightmost index $M(\tilde{m})$ is determined by multiplicities of factors ten, which further split into prime factors five and two. Hence, we have:

$$L(\tilde{m}) = \lfloor \log_{10} \tilde{m} \rfloor - \min(f_5, f_2) + 1$$

where f_5 and f_2 are the multiplicities of prime factors five and two (of $\tilde{m}$). By the properties of $\min$, the above implies:

$$L(\tilde{m}) \geq \lfloor \log_{10} \tilde{m} \rfloor - f_5 + 1$$

From Lemma 1, only the $z_{\tilde{m}}$ term can contain factors of five, and it can have at most $f_5 \leq \lfloor \log_5 2^{p+2} \rfloor$ factors, and so:

$$L(\tilde{m}) \geq \lfloor \log_{10} \tilde{m} \rfloor - \lfloor \log_5 2^{p+2} \rfloor + 1$$

That is, the length $L(\tilde{m})$ grows with the size of the midpoint $\tilde{m}$. By the Maximum Length Theorem 5, Errol1 always prints decimals with 17 digits or less for double-precision numbers, so midpoints $\tilde{m}$ cannot be pathological if:

$$L(\tilde{m}) \geq \lfloor \log_{10} \tilde{m} \rfloor - \lfloor \log_5 2^{54} \rfloor + 1 \geq 17$$

By solving the minimum $\tilde{m}$ for which the above equation holds, we conclude that midpoints larger than 2^{131} *cannot be pathological*.

5.3 Handling Pathological Midpoints

The Pathological Midpoint Theorem 6 guarantees that midpoints are pathological *only if* they fall within a *pathological range* corresponding to midpoints that are *small whole numbers* between $(2^{54}, 2^{131})$ (in our double-precision floating-point setting).

Errol2. Based on these properties, we designed the second iteration of our algorithm Errol2 which behaves as follows. If the input $\hat{v}$ is outside the pathological range, Errol2 converts $\hat{v}$ using the Errol1 algorithm. When the input $\hat{v}$ is in the pathological range $[2^{54}, 2^{131})$, it is possible that one of the adjacent midpoints is pathological. Consequently, Errol2 computes the midpoints $\tilde{m}^-$ and $\tilde{m}^+$ *exactly* as an integer, using well known techniques for binary to decimal conversion for integers [9]. Errol2 then computes the output digits by invoking `digits_hp` (Figure 7) on the exact midpoints. As there is no narrowing, Theorem 3 ensures that the output digits are *correct* and *optimal*.

Empirical Evaluation. Note that Errol2 does *not* guarantee optimal conversion: narrowing *outside* the pathological range *may* still yield a sub-optimal output. However, we ran Errol2 on the sample set of one billion random inputs, and we observed *zero* optimality failures outside the pathological range (and of course, zero inside the range, thanks to the exact midpoints.) Therefore, we have empirically tested Errol2 to have an accuracy of approximately 99.9999999% or better.

6. Errol3: Always Optimal

A 99.9999999% optimality rate is not bad, but why leave anything to chance? Next, we present the final refinement, Errol3, which *guarantees* correct and optimal conversion for all inputs.

Pathological Inputs and Outputs. A *pathological input* is an `FP` value for which the optimal (shortest) decimal is found extremely close to the midpoint (in the uncovered interval) as shown in Figure 1. The decimal output corresponding to a pathological input is called a *pathological output*. Note that the Maximum Length Theorem 5, implies that for double-precision floating-point arithmetic, pathological outputs have *fewer than* 17 digits.

Optimality via Enumeration. Errol3 is founded upon two key insights. First, we identify *necessary conditions*, a set of modular arithmetic constraints, that characterize the midpoints whose neighborhoods contain pathological inputs and outputs (§ 6.2). Second, we provide an efficient algorithm to *efficiently enumerate* all the solutions to the modular arithmetic constraints, thereby tabulating all the possible pathological inputs and their corresponding outputs (§ 6.3). Thus, given an arbitrary $\hat{v}$, Errol3 simply checks if it is one of the pathological inputs and if so, returns its tabulated output. Otherwise, it computes using a modified version of Errol2 (§ 6.4).

6.1 Preliminaries

Our analysis partitions the input space by the (binary) exponent e, *i.e.* into sub-ranges comprising the intervals $[2^e, 2^{e+1})$, which we call the *input range* of e. That is, for a given input range, the exponent e is a fixed constant. For double-precision floating-point numbers, there are 4098 possible exponents e, including subnormal

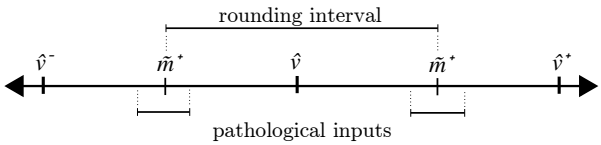

Figure 12: Pathological Input Range. Pathological inputs occur in a small area immediately surrounding the midpoints $\tilde{m}^-$ and $\tilde{m}^+$.

numbers. Our characterization and enumeration algorithm finds all pathological inputs by iteratively searching all possible exponents. In the sequel, we assume a fixed exponent e and its input range, and recall that p denotes the number of bits of precision of the given format.

Enumerating Inputs & Midpoints. The *first* number (resp. midpoint) in the input range is named $\hat{v}_0 = 2^e$ (resp. $\tilde{m}_0 = 2^e + 2^{e-p-1}$.) The *spacing* between floating-point numbers (resp. midpoints) is exactly 2^{e-p}. Therefore, the k^{th} number (resp. midpoint) in the input range, where k is a natural number less than 2^p, is $\hat{v}_k = 2^e + k \times 2^{e-p}$ (resp. $\tilde{m}_k = 2^e + 2^{e-p-1} + k2^{e-p}$).

Pathological Range. The *pathological range* denotes an area around the midpoint $\tilde{m}_k$ that may contain pathological inputs as shown in Figure 12. The size of the pathological range is defined by the *error factor*, and is:

$$(\tilde{m}_k - 2^{e-p}\varepsilon, \tilde{m}_k + 2^{e-p}\varepsilon)$$

Recall that by the Maximum Error Theorem 5, Errol1 has a relative error of at most $79\epsilon^2$. Thus, by setting $\varepsilon \geq 79\epsilon$, the pathological range is guaranteed to cover the amount of error incurred by Errol1 (a factor of ϵ is lost from the factor 2^{e-p}).

Pathological Outputs. A *pathological output* r has the form:

$$\begin{aligned} r &= \tilde{m}_k + \sigma 2^{e-p} = 2^e + 2^{e-p} + k2^{e-p} + \sigma 2^{e-p} \\ &= 2^{e-p-1}(2^{p+1} + 1 + 2k + 2\sigma) \text{ where } |\sigma| < \varepsilon \leq 79\epsilon \end{aligned} \quad (3)$$

A value of $\sigma = 0$ indicates that r is *exactly* a midpoint. By Theorem 6, outside of the pathological midpoint range, r can only be pathological if $\sigma \neq 0$.

Minimal Congruence. The *congruence class* $z \pmod n$ consists of all values $v_k = z + kn$ generated by the integers k. The *minimal congruence*, written $M_c(z, n)$ is the smallest value from the congruence class $z \pmod n$. We write $M_c^+(z, n)$ (resp. $M_c^-(z, n)$) for the *smallest non-negative* (resp. *largest non-positive*) value from the congruence class $z \pmod n$.

6.2 Characterizing Pathologies

To characterize pathological inputs and outputs, we partition the input space into those with (i) *integer* midpoints, *i.e.* inputs greater than 2^{p+1}, and (ii) *non-integer* midpoints, *i.e.* inputs less than 2^{p+1}.

Integer Midpoints. The following theorem provides a *necessary* condition that must hold for an integer midpoint $\tilde{m}_k > 2^{p+1}$ to have a pathological output r in its neighborhood.

Theorem 7 (Integer Midpoints)**.** *A midpoint $\tilde{m}_k > 2^{p+1}$, has a pathological output r in its neighborhood only if*

$$|M_c(\bar{m}_k, 5^n)| \leq \varepsilon 2^{e-p-n}$$

where $n = \lfloor \log_{10} r \rfloor - D + 2$ and $\bar{m}_k = \tilde{m}_k 2^{-n}$.

Proof. First, we show that a pathological output r must be an integer. Suppose not, *i.e.* that r is *not* an integer. Then its right-most index $M(r) < 0$ and its left-most index $N(r) \geq \lfloor \log_{10} 2^{p+1} \rfloor$. Combined, the length $L(r) > \lfloor \log_{10} 2^{p+1} \rfloor + 1$. The Maximum Length Theorem 5 implies that such an r is too long to be optimal. Therefore, a pathological r must be an integer.

As done in the analysis of pathological midpoints, we write the length of r in terms the left-most index and multiplicities of factors

$$L(r) = \lfloor \log_{10} r \rfloor - \min(f_5, f_2) + 1 \leq D - 1$$

where the latter inequality arises from Theorem 5. Thus, we have a lower bound on the number of prime factors two and five:

$$\min(f_2, f_5) \geq \lfloor \log_{10} r \rfloor - D + 2$$

Let n abbreviate $\min(f_2, f_5)$. Then $r \equiv 0 \pmod{2^n 5^n}$ and so

$$r2^{-n} \equiv 0 \pmod{5^n}$$

Based on the definition of a pathological output, σ is an extremely small, non-zero value. As $\sigma \ll 1$, σ is not an integer, which implies that r cannot divide 2^{e-p}. Thus, r divides 2 at most $e - p - 1$ times, or $n \leq e - p - 1$. By the midpoint definition, $\tilde{m}_k$ divides 2^{e-p-1}, and hence, 2^n. Hence, we create the normalized output $\bar{r} = r2^{-n}$ and the normalized midpoint $\bar{m}_k = \tilde{m}_k 2^{-n}$ related by $\bar{r} = \bar{m}_k + \sigma 2^{e-p-n}$. This lets us write $\bar{m}_k$ as a congruence class $\bar{m}_k \equiv -\sigma 2^{e-p-n} \pmod{5^n}$. As σ is bounded by ε (3) there must be a minimal congruence $|M_c(\bar{m}_k, 5^n)| \leq \varepsilon 2^{e-p-n}$. □

Non-Integer Midpoints. The following theorem provides a *necessary* condition that must hold for an non-integer midpoint $\tilde{m}_k \leq 2^{p+1}$ to have a pathological output r in its neighborhood.

Theorem 8 (Non-Integer Range)**.** *A midpoint $\tilde{m}_k < 2^{p+1}$ has a pathological output r in its neighborhood only if*

$$|M_c(\bar{m}_k, 2^n)| \leq \varepsilon 5^{e-p-n}$$

where $n = \lfloor \log_{10} r \rfloor - D + 2$ and $\bar{m}_k = \tilde{m}_k 5^{-n} 10^{-e+p+1}$.

Proof. In order to apply the previous integer techniques, the midpoints $\tilde{m}_k$ are scaled by powers of ten to produce integers

$$\begin{aligned} \tilde{m}'_k &= \tilde{m}_k 10^{-e+p+1} \\ &= 5^{-e+p+1} 2^{p+1} + 5^{-e+p+1} + 2k5^{-e+p+1} \end{aligned}$$

such that $\tilde{m}'_k \in \mathbb{Z}$ (shown by applying the Midpoint Format Definition). By construction, their lengths are equal, *i.e.* $L(\tilde{m}_k) = L(\tilde{m}'_k)$. A pathological output r must have the form

$$r = 2^e + 2^{e-p} + k2^{e-p} + \sigma 2^{e-p}$$

In order to relate r to $\tilde{m}'_k$, we construct a modified output r' as

$$\begin{aligned} r' &= r10^{-e+p+1} \\ &= \tilde{m}'_k + 2\sigma 5^{-e+p} \\ &= 5^{-e+p+1} 2^{p+1} + 5^{-e+p+1} + 2k5^{-e+p+1} + 2\sigma 5^{-e+p} \\ &= 5^{-e+p+1}(2^{p+1} + 1 + 2k + 2\sigma) \end{aligned}$$

so that $L(r) = L(r')$. Using the same reasoning as the Integer Range Theorem, we conclude that r' must be an integer.

Following the same logic as the previous section by substituting the modified output r' for the original r, we obtain the relation

$$\min(f_2, f_5) \geq \lfloor \log_{10} r' \rfloor - D + 2$$

Again, we use the name n for the minimum number of factors of two and five, and obtain the congruence relations

$$r' \equiv 0 \pmod{2^n 5^n} \implies r'2^{-n} \equiv 0 \pmod{5^n}$$

By construction, 5^n must divide r'. Because σ is neither zero nor an integer, r' cannot divide 5^{-e+p+1} implying $n < -e + p + 1$. Because $\tilde{m}'_k$ divides 5^{-e+p+1}, it must also divide 5^n. This fact serves as the basis for creating the normalized output $\bar{r} = r'5^{-n}$ and the normalized midpoint $\bar{m}_k = \tilde{m}'_k 5^{-n}$ which are related by:

$$\bar{r} = \bar{m}_k + \sigma 5^{-e+p-n}$$

This previous equation allows us to write $\bar{m}_k$ as a congruence class

$$\bar{m}_k \equiv \sigma 5^{-e+p-n} \pmod{2^n}$$

As the value of σ is bounded in terms of ε, there must be a minimal congruence such that: $|M_c(\bar{m}_k, 2^n)| \leq \varepsilon 5^{-e+p-n}$ □

6.3 Enumerating Pathologies

Theorems 7 and 8 provide necessary conditions for a midpoint $\tilde{m}$ to have a pathological output in its interval. Consequently we can phrase the problem of enumerating pathological inputs as computing the solutions of a system of pathological constraints.

The Pathological Constraint Problem. Given (1) an arithmetic sequence $\langle m_0, m_1, \ldots \rangle$ whose k^{th} element defined by an initial (normalized midpoint) m_0 and spacing factor α such that $m_k \doteq m_0 + k \times \alpha$; (2) a modulus τ; (3) and a threshold Δ the *pathological constraint problem* is to compute the set of points m_k such that $|M_c(m_k, \tau)| \leq \Delta$.

Exhaustive testing of all midpoints is computationally infeasible for many floating-point formats including double-precision numbers. Instead, we developed an algorithm that finds the (maximal) subsequence of midpoints such that every successive $M_c(m_k, \tau)$ is smaller than the last. In this manner, the algorithm quickly converges on the midpoints that satisfy the pathological constraint.

Offsets. An *offset* is the component of a midpoint that takes the form $x_k = k\alpha$. The offset components form a linear relationship where $x_i + x_j = x_{i+j}$. An offset x_j can be added to a midpoint m_i to form subsequent midpoints $m_i + x_j = m_{i+j}$. There are two elements of the congruence class $m_{i+j} \pmod{\tau}$ of importance: the first real number *above or equal* to $z^+ = M_c^+(m_i, \tau)$ and the first real number *below or equal* to $z^- = M_c^-(m_i, \tau)$. Based on this interpretation, adding x_i can be seen as a *shift upward* to larger real z^+ or a *shift downward* to the smaller real z^-. For a given offset x_j, the downward shift and upward shift are respectively defined as:

$$x_j^- \doteq M_c^-(x_j, \tau) \qquad x_j^+ \doteq M_c^+(x_j, \tau)$$

Using the idea of shifts, the overall goal is restated as: starting at an initial m_0, find an optimal sequence of shifts that generate successive midpoints closer to zero.

Optimal Shift Sequences. The optimal sequence of upward shifts X^+ is defined as the lexicographically smallest subsequence of $\langle x_0^+ \ldots x_N^+ \rangle$ that is decreasing in magnitude; *i.e.*, for any two adjacent elements $x_i^+, x_j^+ \in X^+$, there is no x_k^+ such that $i < k < j$ and $x_i^+ < x_k^+ < x_j^+$. The optimal sequence of downward shifts X^- is similarly defined with respect to sequence $\langle x_0^- \ldots x_N^+ \rangle$.

Optimal Sequence Construction. We begin with the initial sequences $X_0^+ = \langle x_0^+ \rangle$ and $X_0^- = \langle x_0^- \rangle$, and by inductively extending them. Without loss of generality, assume $j \leq k$. Given the two optimal sequences X_k^- and X_j^+, the next element is constructed in the following manner: select the last element $x_j^+ \in X^+$ and select first element $x_a^- \in X_k^-$ such that $x_j^+ + x_a^- > x_k^-$; then, the generated element is the sum $x_z = x_j^+ + x_a^-$. This element x_z represents either a negative shift ($x_z \leq 0$) or a positive shift ($x_z \geq 0$) and is added to the appropriate sequence to create either X_z^+ or X_z^-.

Lemma 2. *Given two upward shifts x_a^+ and x_b^+, the difference $x_c = x_a^+ - x_b^+$ must be either an upward shift if $x_c \in [0, \tau)$ and a downward shift if $x_c \in (-\tau, 0]$. If x_c is zero, it is both an upward and downward shift. Symmetrically for two downward shifts x_a^- and x_b^-, their difference must also be either an upward or downward shift or both.*

Proof. The upward shifts must lie in the range $x_a^+, x_b^+ \in [0, \tau)$, therefore their difference x_c must lie in the range $(-\tau, \tau)$. Symmetrically, the difference between two downward shifts lie in the same range $(-\tau, \tau)$. The difference x_c, falling in the range $(-\tau, \tau)$, is either an upward or downward shift or both. □

Lemma 3. *Given natural numbers j and c such that $j < c$ and shifts x_c^+ and x_j^+ such that $x_c^+ < x_j^+$, then there exists a downward shift $x_{c-j}^- = x_c^+ - x_j^+$. Symmetrically, there exists an equivalent upward shift $x_{c-j}^+ = x_c^- - x_j^-$.*

Proof. By Lemma 2, the resulting shift x_{c-j} must exist and be either a downward or upward shift. Because $x_c^+ < x_j^+$, the shift x_{c_j} must be negative and therefore is a downward shift. The same argument shows that the difference of equivalently defined downward shifts is an upward shift. □

Lemma 4. *Given an arbitrary shift x_c that is not found within the optimal sequence of shifts X, then there exists an optimal shift x_d such that $d < c$ and $|x_d| < |x_c|$.*

Proof. Let x_d be the first element in the optimal sequence X that preceeds x_c. By construction, $d < c$. Assume $|x_d| \geq |x_c|$, then x_c must be an optimal shift and found in X, thus reaching a contradiction. Thus, x_d satisfies the properties of the optimal shift. □

Theorem 9. *If X_k^- and X_j^+ are optimal subsequences then the inductive extensions X_z^- or X_z^+ are also optimal.*

Proof. Without loss of generality, assume x_z is an upward shift. Assume X_z^+ is suboptimal, *i.e.*, there is a x_c^+ such that $j < c < z$ and $x_c^+ < x_j^+$. By Lemma 3, there exists a downward shift $x_{c-j}^- = x_c^+ - x_j^+$. Since $c < z$, the x_{c-j}^- shift occurs earlier than the selected $x_{z-j}^- = x_a^-$ shift. If x_{c-j}^- is in X^-, then the algorithm failed to select the *first* available downward shift, thus reaching a contradiction. If x_{c-j}^- is not in X^-, then by Lemma 4 there exists an optimal shift x_p^- in X^- that the algorithm failed to select, thus reaching a contradiction. □

Midpoint Search. The midpoint search begins at the initial midpoint m_0 and is performed inductively. Given a midpoint m_k that is positive, we select the first offset $x_i^- \in X^-$ such that the next midpoint $m_{k+i} = m_k + x_i^-$ is closer to zero $|M_c(m_{k+i}, \tau)| < |M(m_k, \tau)|$.

Theorem 10. *After the midpoint m_k, the generated midpoint m_{k+i} is the first midpoint whose minimal congruence is closer to zero.*

Proof. By construction, any different shift from X^- would create a midpoint with too large or small a minimal congruence. Suppose there exists a larger shift x_c *not in* X^- that creates a midpoint satisfying the condition $|M_c(m_{k+c}, \tau)| < |M(m_k, \tau)|$. Based on this construction, c must be larger than i (in order to preserve the optimal sequence definition), which indicates that m_{k+c} is not the first midpoint closer to zero. By contradiction, the midpoint m_{k+i} is the first such midpoint. □

Symmetrically, if m_k is negative, we select the first offset $x_i^+ \in X^+$ such that the next midpoint is nonpositive. In this manner, we generate a sequence of midpoints that "ping-pong" back and forth across zero, always decreasing in magnitude. In the event that a midpoint satisfying $|M(m_k, \tau)| \leq \varepsilon$ is found, the above process no longer applies; instead, midpoints are more exhaustively searched by performing *all* shifts that land within the range $[-\varepsilon, \varepsilon]$. This ensures that all midpoints satisfying midpoints are found.

Handling Subnormals. Because the above has assumed an arbitrary floating-point format with p bits of precision, subnormal numbers are easily encoded by modifying the value of p based on the exponent e. In this manner, the enumeration algorithm searches the subnormal number ranges for pathological inputs.

6.4 Guaranteeing Optimal Conversion

Before running the enumeration algorithm, the underlying algorithm of Errol2 was modified to remove narrowing and widening. Remember, the purpose of narrowing (and widening) is to guarantee the algorithm always generates a correct (or optimal) result. This step is no longer necessary for Errol3 since all suboptimal or incorrect results are *enumerated a priori*. Hence, Errol3 obtains a performance benefit because verifying outputs at runtime is *no longer necessary*.

After removing the narrowing and widening steps, we used the enumeration algorithm to generate a list of *possibly* incorrect or suboptimal inputs. Each input was run using Errol2 to enumerate a *complete* list of inputs that do not generate correct and optimal outputs. In total, we found that only 45 inputs (of the nearly 2^{64} inputs) generate incorrect or suboptimal results; all other inputs are guaranteed to generete correct and optimal output. In order to correctly and optimally handle the failing inputs, they are hard-coded into a lookup table that maps the failing inputs to correct and optimal outputs. Combining the special handling of integers and this lookup table, Errol3 is guaranteed to be *correct and optimal without runtime checks*.

7. Performance Evaluation

Next, we evaluate the performance of Errol3 with the goal of comparing it against previous state of the art algorithms.

Methodology. Our experiment compares Errol3, Grisu3, and an updated version of Dragon4. For each algorithm, we measure performance by recording the time in clock cycles taken to convert a floating-point representation to a decimal string. Inputs are randomly generated IEEE-754 double-precision floating-point numbers. Outputs consist of a decimal string significand and an integer exponent. All experiments were performed on an Intel(R) Core(TM) i7-3667U CPU at 2.00GHz running Xubuntu Linux 14.04 and compiled with gcc 4.8.2. Each algorithm is tested using 20,000 random inputs with each input converted 100 times, of which the median 80 values were averaged to compute the final result. The source code can be downloaded at https://github.com/marcandrysco/Errol. The performance numbers are shown in Figure 13, which we look at part by part.

Errol3 across all inputs. Figure 13(a) shows the performance of Errol3 in isolation. We can see that its performance across the input space is fairly constant, except for three anomalies. First, Errol3 incurs a slowdown for values larger than 10^{291}. This is caused by the fact that the lookup table for powers-of-ten can only store numbers down to 10^{-291}, and so inputs above that point must be normalized by iteratively dividing by ten, incurring a performance penalty. Second, Errol3 incurs two slowdowns for values smaller than 10^{-292}. This is caused by significant processor slowdowns when operating on subnormal numbers, and the powers-of-ten lookup table can only store numbers down to 10^{-308}. Finally, there is a sizable performance anomaly for numbers in the range 2^{53} to 2^{131}. These are the numbers converted using the integer algorithm which only applies to numbers in that range (§ 5.3).

Errol3 vs. Grisu3. Figure 13(b) compares the performance of Grisu3 (in black) and Errol3 (in grey). Across the entire input space, Errol3 is, on average, $2.4\times$ slower than Grisu3.

Errol3 vs. Dragon4. Figure 13(c) shows Dragon4 (in black) and Errol3 (in grey). Furthermore, we can also see that the performance of Dragon4 varies significantly across the input space, forming a "V" shape that increases linearly as numbers get further away from 0. In contrast, both Errol3 and Grisu3 have much less variation in performance across the input space. Across the entire input space, Errol3 is, on average, $5.2\times$ faster than Dragon4.

Errol3 vs Grisu3-with-fallback. Finally, because Grisu3 fails to generate optimal outputs for approximately 0.5% of inputs, we consider a version of Grisu3 which falls back to Dragon4 when Grisu3 fails to generate an optimal output. Figure 13(d) shows this "Grisu3 with fallback" (in black) and Errol3 (in grey). On average, Errol3 is $2.4\times$slower than Grisu3 with fallback.

Performance across Architectures. As Errol3 uses floating-point operations instead of the integer operations used by Grisu3 and Dragon4, its performance compared to those algorithms is dependent on the relative speed of the floating-point operations versus integer operations on a given architecture. Thus, testing Errol3 on a variety of architectures produced an appreciable variation in performance numbers. For example, relative to Dragon4, we observed results ranging from the $5.2\times$ speedup on an Intel(R) Core(TM) i7-3667U to a $5.8\times$ on an Intel Xeon X5660.

8. Related Work

Coonen published an implementation guide for IEEE-754 floating-point arithmetic detailing an early binary-to-decimal conversion algorithm [2], and later expanded on conversion algorithms, covering both correctly rounded and "imperfect" conversions [3].

Steele and White published a paper for printing-floating point numbers that detailed their Dragon4 algorithm [14]. Dragon4 provided strong guarantees that the output is both correct and optimal, a process that utilized large integer arithmetic. Later work by Gay [5] and Burger [1] provided performance improvements over the vanilla Dragon4 algorithm.

Loitsch published the Grisu3 algorithm, introducing a fast conversion method that guarantees correct but possibly suboptimal output [10]. Unlike previous work, he established a method for verifying the output, and in the 0.05% of cases when the result is suboptimal, the algorithm returns a flag indicating failure. Although Grisu3 significantly outperforms Dragon4 and its successors, Grisu3 still relies on predecessor algorithms as a fallback when it fails to generate optimal outputs.

The use of high-precision floating-point data types consisting of multiple, non-overlapping components can be found in previous literature by Knuth [9], Dekker [4], Priest [12], and Shewchuk[13]. Previous research by Hida [7] has demonstrated algorithms for supporting a large range of arithmetic operations on floating-point numbers consisting of up to four double-precision numbers.

Acknowledgements

We thank the anonymous reviewers for this paper and for a previous version, for their invaluable feedback and suggestions, in particular, for providing a reference to David Matula's In-and-out Conversions [11] which greatly simplified the proof of the Maximum

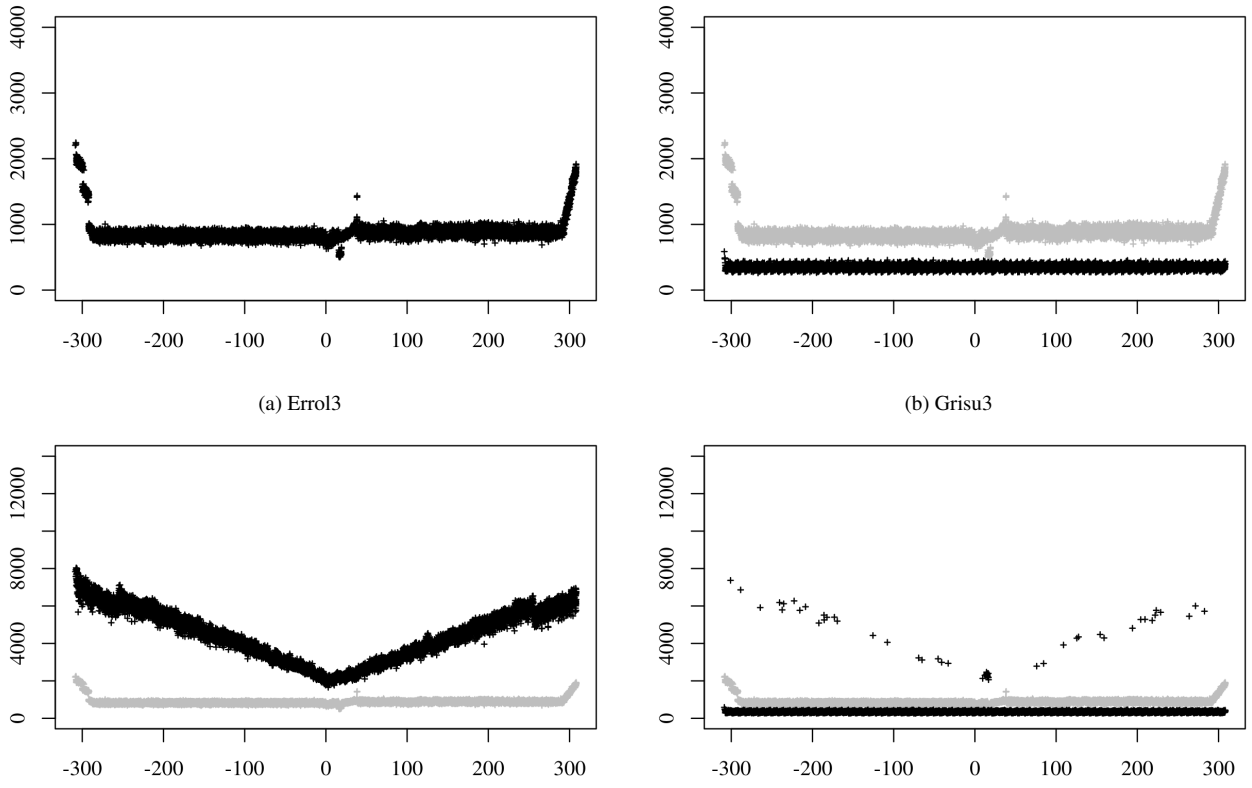

(a) Errol3

(b) Grisu3

(c) Dragon4

(d) Grisu3 with fallback to Dragon4

Figure 13: Performance results, shown in black, for (a) Errol3 (b) Grisu3, (c) Dragon4 and (d) Grisu3 with fallback to Dragon4. Plots (b), (c), and (d) also show Errol3 in grey for reference. Each point plots a single value tested against all algorithms; the x-axis provides the magnitude of the value and the y-axis gives the number of clock cycles required to complete the conversion.

Length Theorem. This work was supported by NSF grant CNS-1514435 and a generous gift from Microsoft Research.

References

[1] R. G. Burger and R. K. Dybvig. Printing floating-point numbers quickly and accurately. In *PLDI*, 1996.

[2] J. T. Coonen. An implementation guide to a proposed standard for floating-point arithmetic. *IEEE Computer*, 13(1), 1980.

[3] J. T. Coonen. *Contributions to a Proposed Standard for Binary Floating-point Arithmetic (Computer Arithmetic)*. PhD thesis, 1984.

[4] T. Dekker. A floating-point technique for extending the available precision. *Numerische Mathematik*, 18(3), 1971.

[5] D. M. Gay. Correctly rounded binary-decimal and decimal-binary conversions. In *Numerical Analysis Manuscript*. 1990.

[6] D. Goldberg. What every computer scientist should know about floating-point arithmetic. *ACM Comput. Surv.*, 23(1), 1991.

[7] Y. Hida, X. S. Li, and D. H. Bailey. Algorithms for quad-double precision floating point arithmetic. In *Symp. on Computer Arithmetic*, 2001.

[8] W. Kahan. Pracniques: Further remarks on reducing truncation errors. *Commun. ACM*, 8(1), 1965.

[9] D. E. Knuth. *The Art of Computer Programming, Volume II: Seminumerical Algorithms, 2nd Edition*.

[10] F. Loitsch. Printing floating-point numbers quickly and accurately with integers. In *PLDI*, 2010.

[11] D. W. Matula. In-and-out conversions. *Commun. ACM*, 11(1), 1968.

[12] D. M. Priest. *On Properties of Floating Point Arithmetics: Numerical Stability and the Cost of Accurate Computations*. PhD thesis, 1992.

[13] J. R. Shewchuk. Adaptive precision floating-point arithmetic and fast robust geometric predicates. *Discrete & Computational Geometry*, 18: 305–363, 1996.

[14] G. L. Steele and J. L. White. How to print floating-point numbers accurately. In *PLDI*, 1991.